

PECULIARITIES OF THE FORMATION OF AEROSOL FIELD VERTICAL STRUCTURE OVER TOMSK IN SUMMER OF 1995

Yu.S. Balin and A.D. Ershov

*Institute of Atmospheric Optics,
Siberian Branch of the Russian Academy of Sciences, Tomsk*

Received December 27, 1995

The peculiarities are discussed of the formation of aerosol field vertical structure derived from an analysis of variations of the scattering coefficients averaged over the period of observation and the altitude behavior of the autocorrelation matrices. Experimental data were obtained in laser sounding of the atmosphere at altitudes up to 1.5–2 km in the daytime in June and July of 1995. Differences were revealed in the diurnal behavior of the scattering coefficients and the degree of their vertical correlation within these months. They can be explained by synoptic conditions and type of observed air masses.

As is well known, the bulk of the atmospheric aerosol characterized by the widest spatial and temporal variability is concentrated in the lower layers of the atmosphere. The vertical structure and optical characteristics of aerosol fields are formed under effects of many physical processes of different temporal and spatial scales, from micrometeorological to synoptical range of the spectrum.

Geophysical factors caused by synoptic processes accompanied with change of air masses produce comparatively slow effect. Diurnal variations of thermal state of the atmosphere are much faster. In their turn, these processes determine the dynamics of appearance and dissipation of temperature inversions and the diurnal behavior of the relative humidity of air directly affecting the aerosol optical characteristics.

The experimental bases for the study of the vertical structure of aerosol fields now provide airborne local sensors^{1,2} and laser sounding of the atmosphere.^{3,4}

The aim of this paper is lidar investigation of the behavior of the vertical profiles of the aerosol scattering coefficient in the lower troposphere at different times of the day under varying synoptic conditions.

The profiles of the scattering coefficient were measured with the LOZA-3 scanning single-frequency lidar⁵ at a wavelength of 0.53 μm in the daytime in June and July of 1995.

The lidar was placed on a hill on the east outskirts of Tomsk, which made it possible to carry out the sounding of the atmosphere both in vertical direction and at different zenith angles. To do this, the coordinates of the paths of sounding, corresponding to elevation angles of 1, 40, and 80° (in the direction toward the city) and, after crossing the vertical, 80, 40, 20, and 2° (in the opposite direction toward forest areas), were inputted into the computer memory. Such a scheme of the experiment helped us to provide

monitoring of the effect of pollutants of industrial origin.

Measurement runs were performed in the daytime every 2 hours from 8 a.m. to 8 p.m. Thus, seven vertical profiles of aerosol scattering coefficient were recorded during a day and the data array of 160 samples was obtained during all period of observations.

The lidar recorded the vertical stratification of aerosol fields at distances up to 2–3 km in horizontal direction and up to 1–2 km at angles close to the zenith. The maximum range of sounding increased up to 5–7 km in the case of appearance of clouds. Spatial resolution was 7.5 m and angular resolution was 10'.

Each act of sounding was formatted as an individual file with the corresponding rated and service data (date, time, characteristics of the path, spatial resolution, etc.).

Let us briefly consider the peculiarities of synoptic and meteorological conditions of the atmosphere during the experiment.

Temporal behavior of the principal meteorological parameters such as temperature (T), relative humidity (f), wind speed and direction (W and θ), as well as the scattering coefficient (σ) measured in the ground layer of the atmosphere with a path photometer at a wavelength of 0.5 μm is shown in Fig. 1. The temporal diagram of the peculiarities of synoptic conditions is shown in Fig. 2. As is seen from the diagram, the weather during this period was determined by the Arctic and temperate air masses. During the first half of June the major portion (60%) of air masses was the Arctic air mass and hence the portion of the temperate air mass was 40%. The portion of the temperate air mass in July was increased up to 57% and the portion of the subtropical air mass was increased up to 18%. The portion of the Arctic air mass was decreased down to 36%.

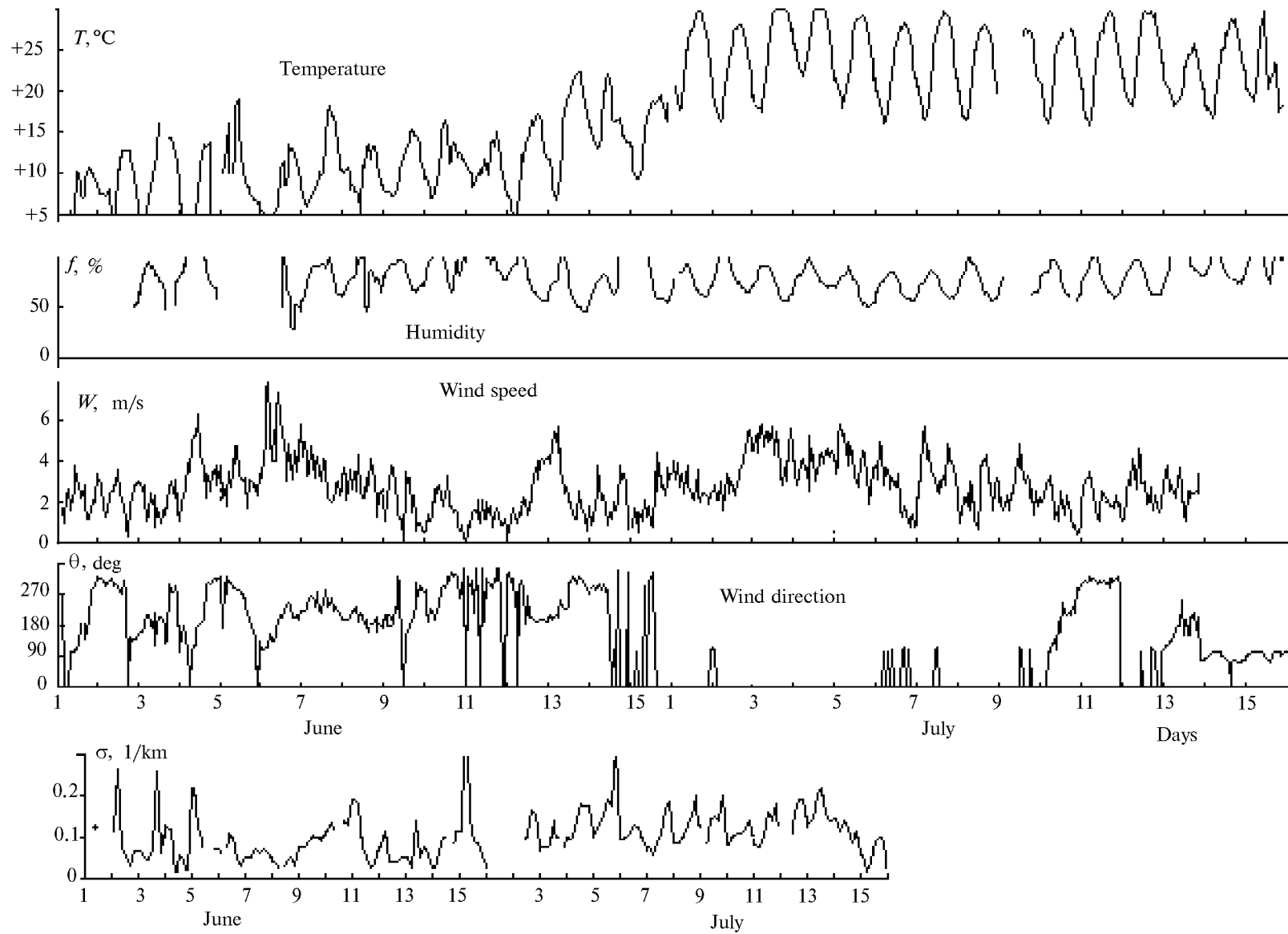


FIG. 1. Temporal behavior of the principal meteorological parameters in June and July of 1995.

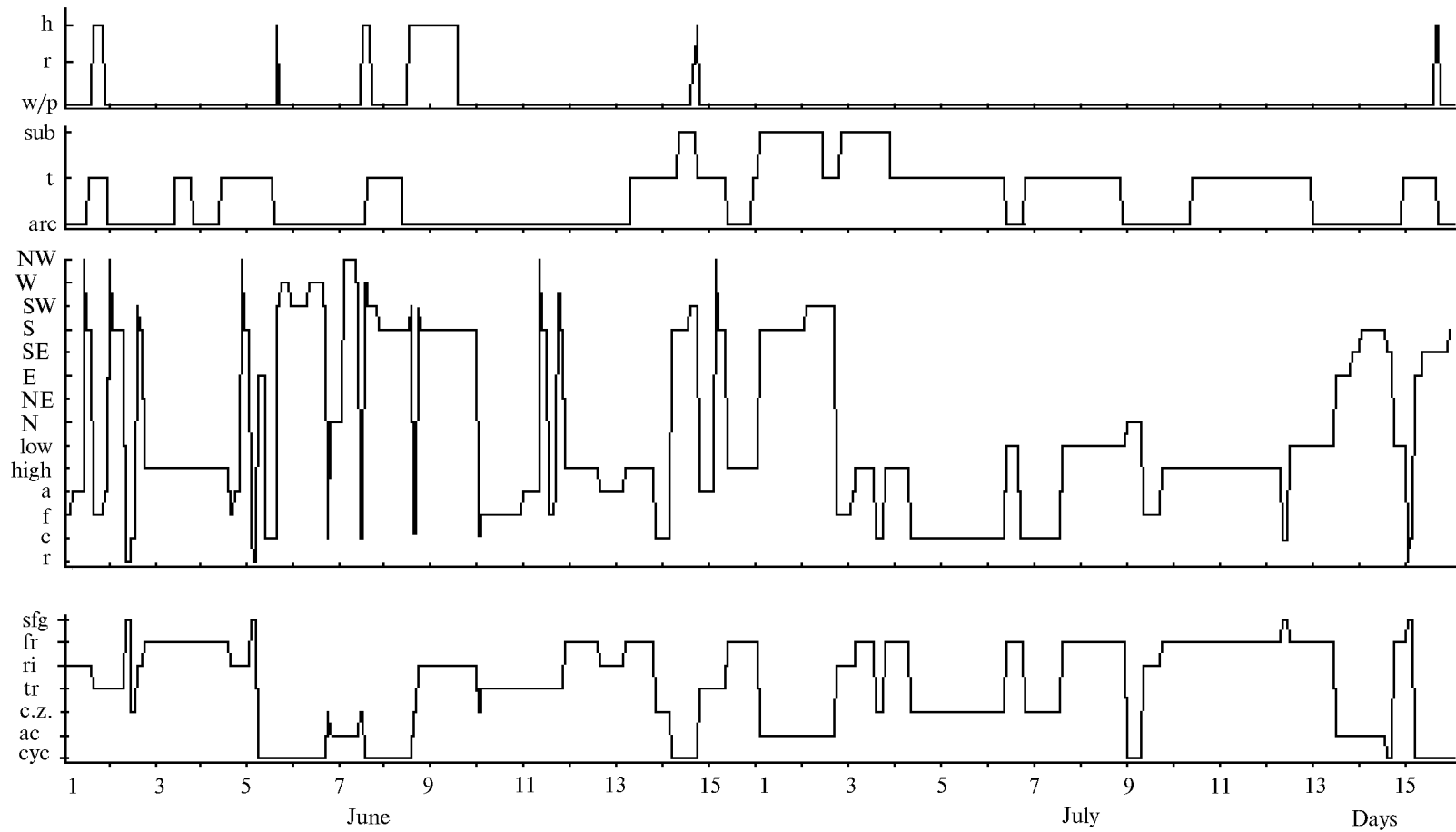


FIG. 2. Temporal diagram of synoptic conditions in June and July of 1995. Here, h denotes hail, r denotes rain, w/p means without peculiarities, sub is for subtropical type of air mass (TAM), t denotes temperate TAM, arc is for the Arctic TAM, NW is for northwest, W is for west, SW is for southwest, S is for south, SE is for southeast, E is for east, NE is for northeast, N is for north, low denotes low pressure, high denotes high pressure, a denotes axis, f denotes fore, c denotes center, r denotes rare, sgf denotes small-gradient field, fr denotes front, ri denotes ridge, tr denotes trough, c.z. denotes contrast zone, ac denotes anticyclone, and cyc denotes cyclone.

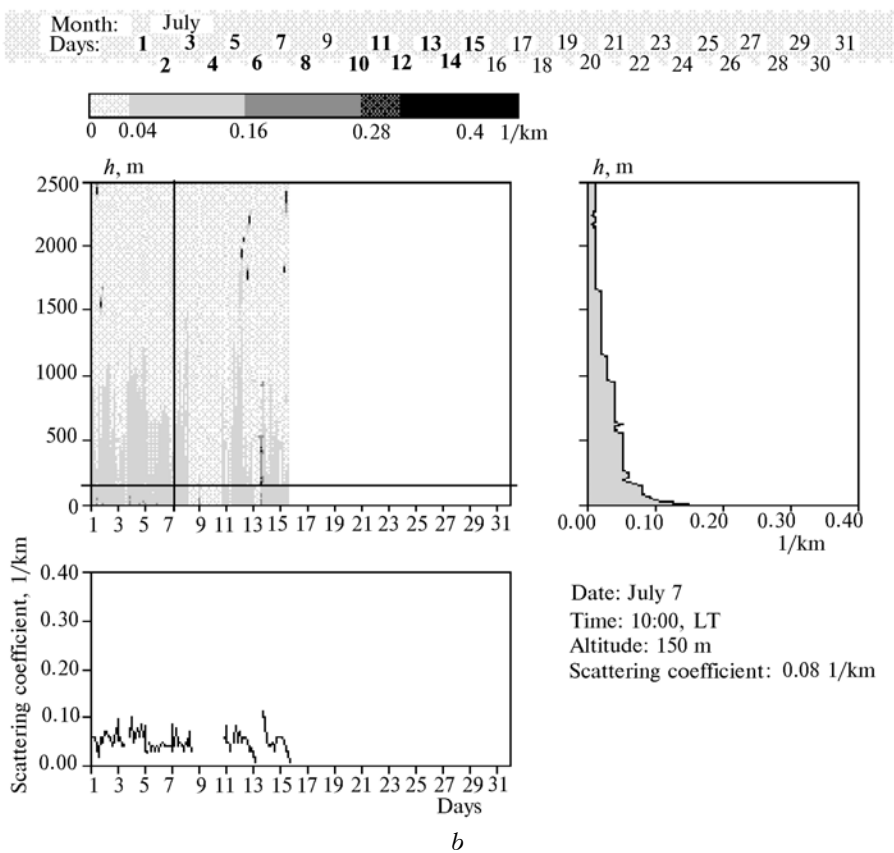
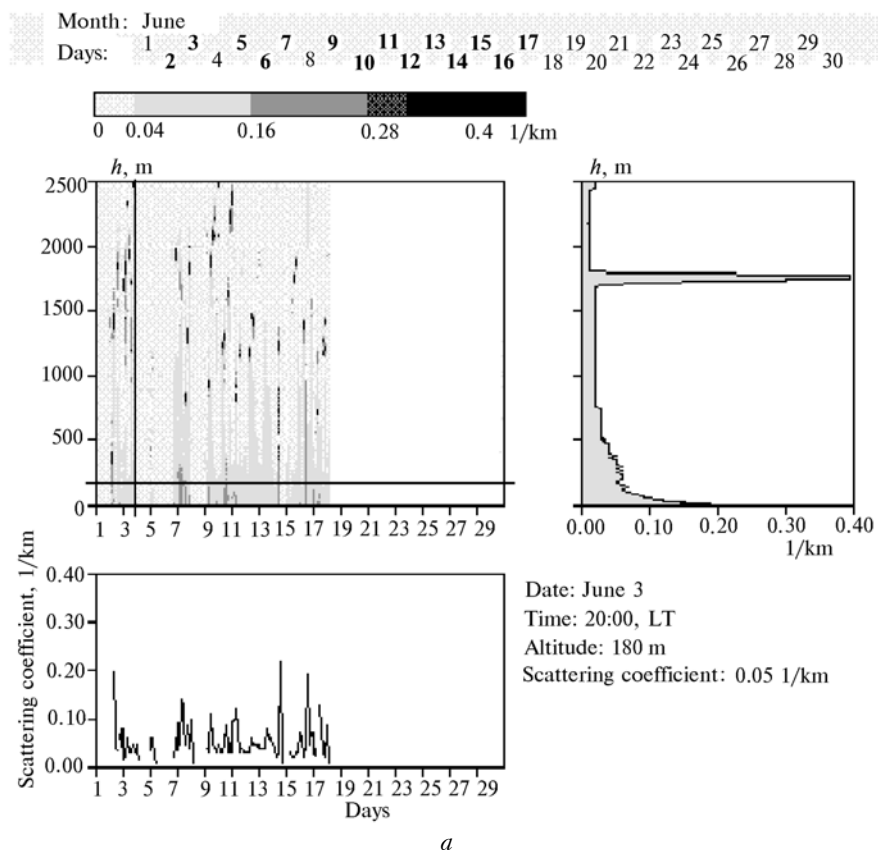


FIG. 3. General pattern of the scattering coefficient profiles: a) June, b) July.

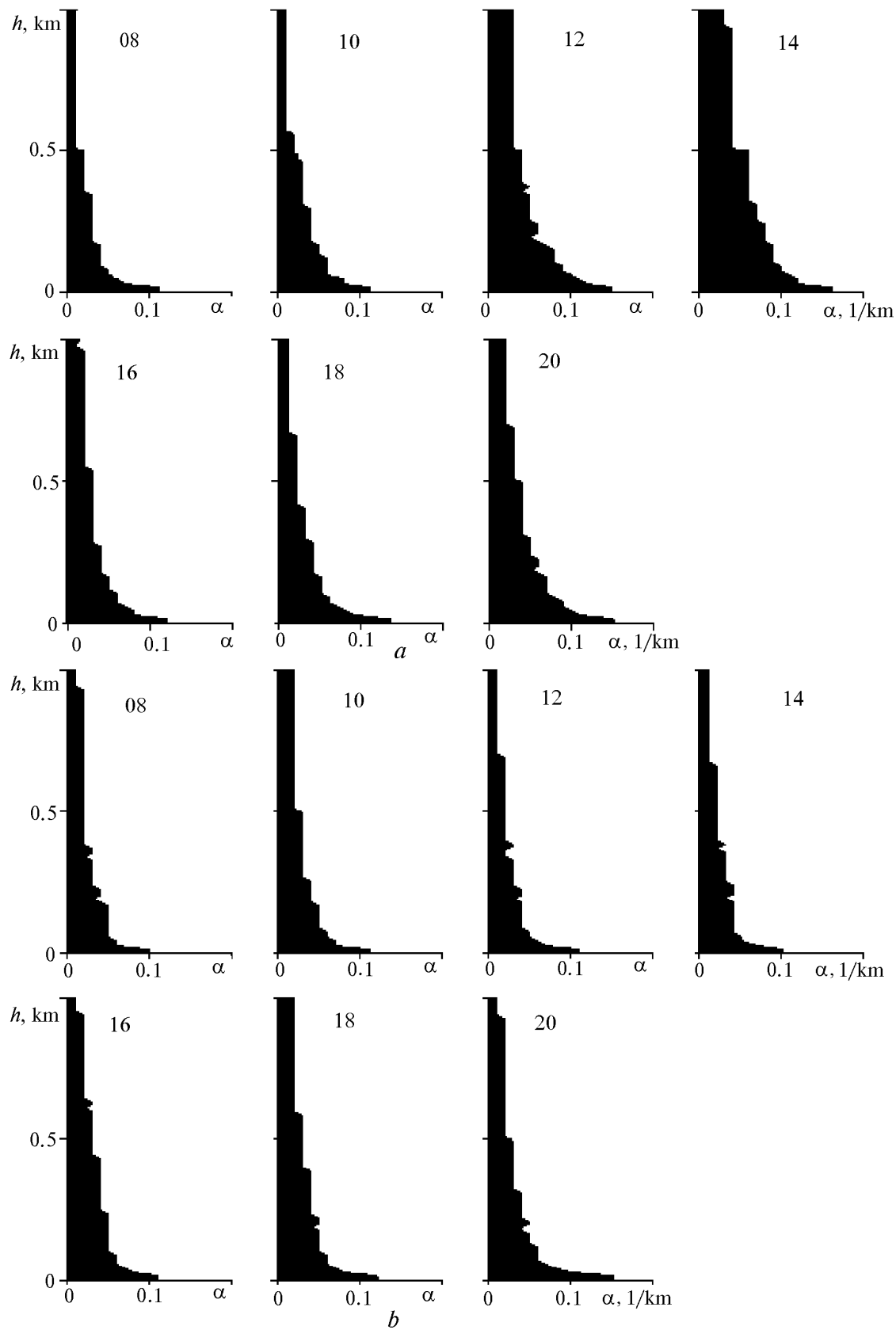


FIG. 4. Average diurnal behavior of the scattering coefficient: a) June, b) July.

According to the data of long-term observations in Western Siberia, the major contribution (~60%) to the formation of synoptic situations came from the continental temperate air mass.⁶ Classification of air masses in July corresponded to the above-noted statistics. But in June the Arctic air mass was prevalent. This explains almost everyday fall of precipitation and small relative portion of cloudless days. Though the synoptic diagram does not show (the upper part of Fig. 2), it is clearly seen from the lidar data shown in Fig. 3a in generalized form. The days when the measurements were carried out are indicated in the upper part of the figure. The format of data recording makes it possible to retrieve the data on the profile of the scattering coefficient for any day of measurements (at the right of the figure) and at any altitude during all period of measurements (at the bottom of the figure) by means of moving the cursors in vertical and horizontal directions. The values of the scattering coefficient are displayed as gradations in blackening in the upper part of the figure. As is seen from the data, the black fragments corresponding to clouds are observed in practically any day of measurements. The altitude range for clouds is between 1000 and 2000 m. Another pattern was observed in July (Fig. 3b). Clouds were practically absent in the above-indicated altitude range, and precipitation was observed only on the last day of measurements.

The diurnal behavior of the vertical profile of the scattering coefficient averaged over all period of measurements in June and July of 1995 is shown in Figs. 4a and b, respectively. On the whole, the patterns of the behavior of profiles in these months were identical. As could be expected, the largest gradient was observed in the lowest layer of the atmosphere extending up to 150 m. Then the gradient of the scattering coefficient smoothly decreased at altitudes up to 500–700 m, and further its values remained practically constant.

As to the diurnal behavior of the scattering coefficient, the increase of the scattering coefficient was observed in June near noon. This should be explained by the change of the diurnal thermal regime of the atmosphere.

We have already observed such behavior of the scattering coefficient earlier when we implemented the SATOR-93 program⁷ (April–June of 1993). This implies a certain degree of stability of the formation of the vertical structure of aerosol field in the seasons under study.

At the same time, there were some differences in the diurnal behavior in comparison with the data of SATOR-93 (comparison with this period was carried out because it was provided with sufficient statistics, namely, about 700 measurements were carried out). It was noted in Ref. 7 that the aerosol content in the

lower layers of the atmosphere was increased from April to June, i.e., as the air temperature increased.

A reverse tendency was observed in 1995. Though the air temperature (Fig. 1) in July was approximately twice higher, the values of the scattering coefficient at noon and 2 p.m. in June exceeded the analogous values in July. If higher temperature had provided the more active turbulent regime and better mixing of the aerosol along the vertical direction, it would have resulted in the increase of the absolute value of the scattering coefficient in the lower atmospheric layers. Nevertheless, this was not the case. To explain this fact, let us analyze the autocorrelation matrices of aerosol scattering coefficients in different periods of measurements.

The autocorrelation matrices obtained in April–June of 1993 (Ref. 8) are shown in Fig. 5a. It is seen how the shapes of correlation dependence change from spring to summer measurements. The vertical behavior of variation of all correlations in April is approximately the same, but the shape of the autocorrelation matrix in June has a specific character. Namely, crowding of curves corresponding to a correlation coefficient of 0.5 was observed near the 1300-m altitude. Thus, the altitude range appeared inside this altitude interval, where the values of the scattering coefficient were well correlated. One also should pay attention to the presence of the layer 300 m thick adjoining its boundary from above. The anomalous behavior of the correlation coefficient, consisting in its increase for all curves, was observed here. This layer is called the entrainment layer in the literature³ and we will not consider it in this paper.

A common feature of the matrices presented here is their correlation in the layer extended up to 600 m, at the boundary of which the coefficient $R(\sigma_0, \sigma_h)$ reaches 0.5 independently of the month of measurements.

The autocorrelation matrices obtained in summer of 1995 had the same shapes (Fig. 5b). The crowding of lines by the criterion $R(\sigma_i, \sigma_k) = 0.5$ was also observed, that made it possible to identify the characteristic altitude ranges of aerosol mixing. The value of $R(\sigma_0, \sigma_h)$ in June of 1995 was first equal to 0.5 at an altitude of 600 m too. However, further the correlation fluctuated near this value up to 1.3 km, as we have already mentioned when analyzing the data of 1993, rather than decreased. In spite of the visual similarity, the autocorrelation matrix observed in July had another numerical values. The altitude where $R(\sigma_0, \sigma_h) = 0.5$ was slightly lower here ($h = 500$ m) and the height of the mixing layer was also smaller ($h = 900$ m).

By and large patterns of the behavior of the autocorrelation matrices in summer of 1993 and 1995 were similar.

What will be the form of these matrices, if we classify them according to the type of air mass?

To answer this question, let us consider Fig. 6a, where the autocorrelation matrices for Arctic and temperate air masses of 1993 are shown. Whereas the pattern of the behavior remained practically

unchanged for the temperate type of air mass that determined the weather in June, the differences were significant for the Arctic air mass. The height of the mixing layer here did not exceed 600 m, and all curves $R(\sigma_0, \sigma_h) = 0.5$ inside this layer were grouped at this altitude.

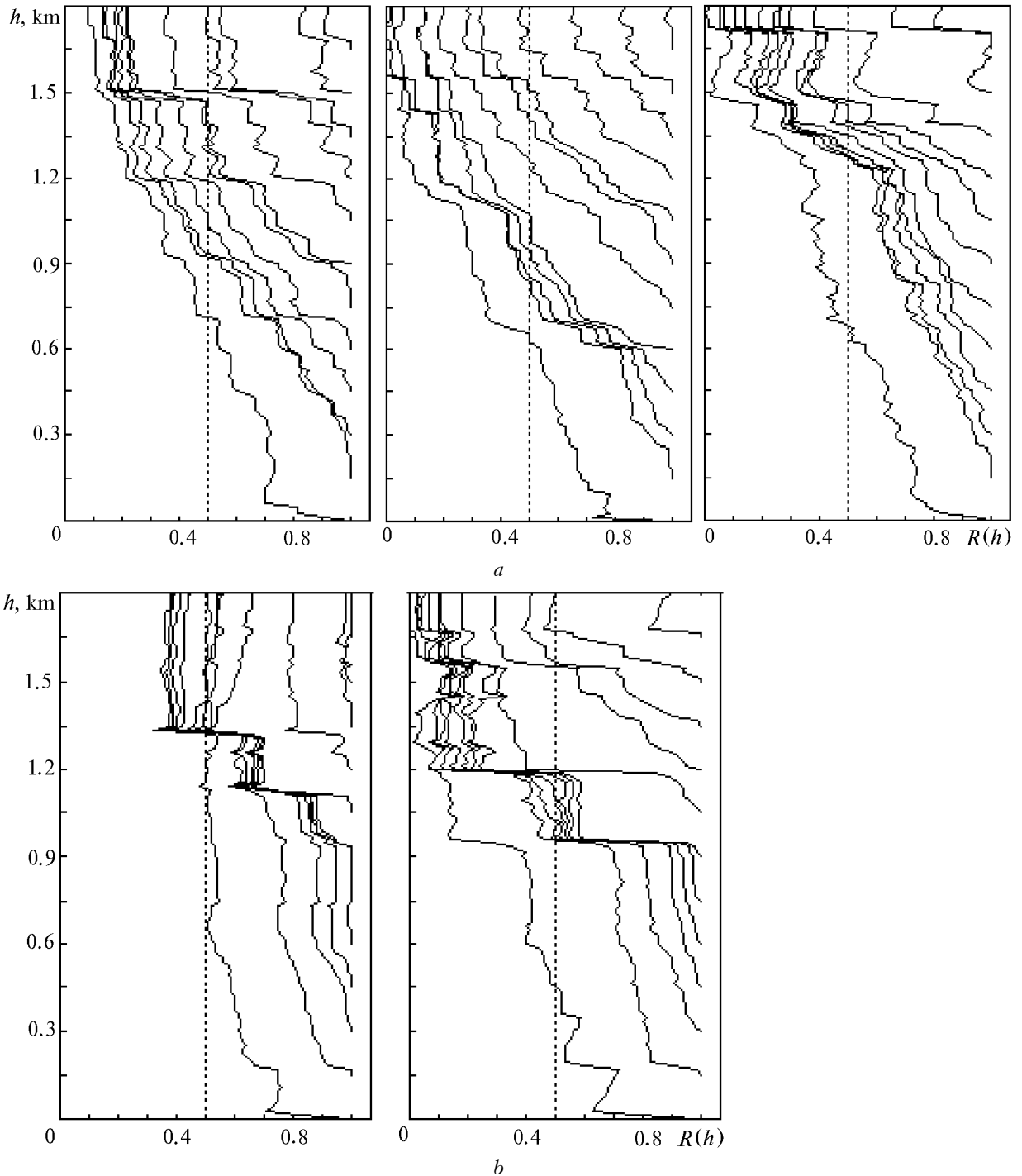


FIG. 5. Autocorrelation matrices of the scattering coefficient: a) 1993, b) 1995.

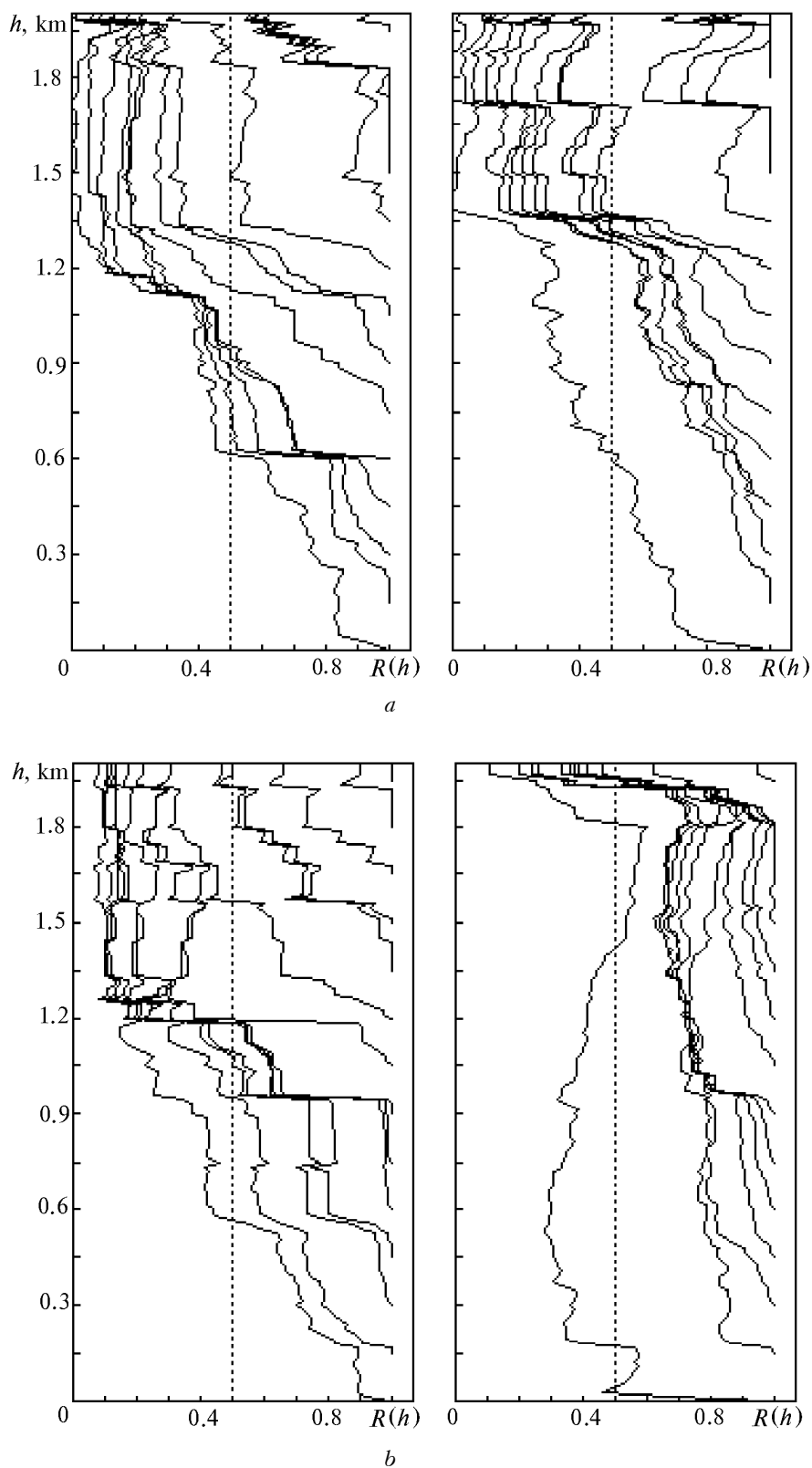


FIG. 6. Autocorrelation matrices for different types of air masses: left figures are for Arctic and right – for temperate air masses in 1993 (a) and 1995 (b).

Analogous classification was done for the bulk of data of 1995. The results are shown in Fig. 6b. As is seen from the figure, the differences are first of all in the behavior of the autocorrelation matrix between the ground level and higher altitudes for the temperate type of air mass. The values of the autocorrelation function are so small that one can say about the absence of exchange by air masses between the lower and higher altitudes. At the same time, the values of the correlation coefficients are high starting from 200 m up to 1.8 km.

One should explain the obtained result by the peculiarities of free convection in the boundary layer of the atmosphere and by the behavior of the height of the mixing layer. These peculiarities are caused by the temperature difference between the underlying surface and the adjoining air layer. As was noted in Ref. 9, "the arrangement of the types of air masses in order of increasing height of the mixing layer coincides with the subsequent change of their temperature effect on the surface," i.e., the warmer is the air, the thinner is the mixing layer, so convection is not developed. According to these data,⁹ the situation is dramatized in the front zones where the most unfavorable conditions for aerosol spreading along the vertical direction arise from the viewpoint of the thermal structure. The height of the mixing layer decreases down to 200 m. As it follows from Fig. 2, the relative contribution of fronts in July was about 30% according to our data.

Evidently, it is this mechanism that explains the diurnal behavior of the scattering coefficients in July (Fig. 4b), where the typical increase of the values at high altitudes near noon was not observed.

It should be noted that an analysis of the autocorrelation matrices aimed at determining the height of the mixing layer by the criterion $R(\sigma_0, \sigma_h) = 0.5$ was first made in Refs. 1 and 2 in

processing of the data of airborne measurements with the local sensors.

ACKNOWLEDGMENTS

In conclusion, we note that the experimental investigations were carried out as part of the SATOR-95 program. The authors thank the participants of this program for the possibility of using the results of joint measurements.

The work was done under financial support of Russian Foundation of Fundamental Researches (Grant No. 94-05-16461-a).

REFERENCES

1. M.V. Panchenko and S.A. Terpugova, *Atmos. Oceanic Opt.* **7**, No. 8, 552-557 (1994).
2. B.D. Belan, *Atmos. Oceanic Opt.* **7**, No. 8, 558-562 (1994).
3. Y. Sasano, *J. Meteorol. Soc. Japan* **63**, 419-435 (1985).
4. R. Boers, E.W. Eloranta, and R. L. Coulter, *J. Climate Appl. Meteorol.* **23**, No. 2, 247-266 (1984).
5. Yu.S. Balin and I.A. Razenkov, *Atmos. Oceanic Opt.* **6**, No. 2, 104-114 (1993).
6. S.D. Koshinskii, ed., *Climate of Tomsk* (Gidrometeoizdat, Leningrad, 1982), 176 pp.
7. Yu.S. Balin, A.D. Ershov, and I.A. Razenkov, in: *Abstracts of Reports at the Second Interrepublic Symposium on Atmospheric and Oceanic Optics*, Tomsk (1995), Part 2, pp. 322-323.
8. Yu.S. Balin, A.D. Ershov, and I.A. Razenkov, *ibid.*, pp. 272-273.
9. M.A. Lokoshchenko, B.A. Semenchenko, M.A. Kallistratova, and M.S. Pekur, *Atmos. Oceanic Opt.* **7**, No. 7, 522-527 (1994).